Biochemistry

 Volume 37, Number 5 February 3, 1998

Accelerated Publications

Effect of Pressure on Individual Hydrogen Bonds in Proteins. Basic Pancreatic Trypsin Inhibitor†

Hua Li, Hiroaki Yamada, and Kazuyuki Akasaka*

Division of Molecular Science, The Graduate School of Science and Technology, and Department of Chemistry, Faculty of Science, Kobe University, 1-1 Rokkodai-cho, Nada-ku, Kobe 657, Japan

Received September 15, 1997; Revised Manuscript Received November 20, 1997

ABSTRACT: By performing two-dimensional ^{1}H NMR measurements at 750 MHz at varying hydrostatic pressure (1−2000 bar) in an aqueous environment (90% ^1H_2O/10% ^2H_2O), we found that the signals of the peptide NH protons of basic pancreatic trypsin inhibitor (BPTI) in the folded state shift their positions linearly and reversibly with pressure. The strong tendency for low-field shifts of these protons indicates that most of the amide groups form hydrogen bonds either with carbonyls or with water and that these hydrogen bonds are shortened by pressure. The NH protons interacting favorably with solvent water tend to exhibit larger pressure-induced shifts than others, showing that the shift can be used as a diagnostic probe for the hydrogen bonding state of an NH group with water. Furthermore, we estimated shortening of individual H···O distances of the NH···O═C hydrogen bonds at 2000 bar on the basis of the empirical shift−distance correlation for BPTI. The estimated shortened distances varied considerably from site to site in the range of 0−0.11 Å, larger in the turn but smaller in the interiors of secondary structures. These variations suggest that the volume fluctuation is heterogeneous within BPTI and that high-pressure NMR at high field can offer a unique opportunity for detecting microscopic structural fluctuation in proteins.

Pressure has long been known to affect functions of proteins and living organisms (*1*−*4*). Origins of these effects must be sought in the alteration of functional structures and dynamics of proteins by pressure. To date, evidence for pressure-induced changes in functional structures of proteins has been obtained either macroscopically from measurements of compressibility (*5*, *6*) or microscopically from measurements of optical (*7*, *8*), vibrational (*9*), and NMR[1] spectra (*10*−*13*) using local structural probes. Only in one case, structural changes were reported at an atomic scale detail over an entire protein molecule based on the X-ray diffraction method (*14*).

We have recently introduced an alternative technique capable of reporting at the microscopic level structural changes in a folded protein, namely high-pressure NMR spectroscopy at high resolution (*15*). The essential part of this technique is an on-line variable-pressure quartz cell that can fit to a commercial NMR probe on a modern NMR spectrometer, operating at a high magnetic field (17.6 T or 750 MHz for proton). Using this technique, we have recently demonstrated in hen lysozyme that the hydrophobic core is the region of a preferential compressibility (*16*). This finding is consistent with the hitherto admitted notion that the major contribution to the compressibility of a folded protein arises

† This work was supported by Grants-in-Aid for Scientific Research 09480177 and 09261224 from the Ministry of Education, Science, Sports and Culture of Japan.

* To whom correspondence should be addressed. E-mail: akasaka@kobe-u.ac.jp.

[1] Abbreviations: BPTI, bovine pancreatic trypsin inhibitor; NMR, nuclear magnetic resonance; TOCSY, total correlation spectroscopy; NOESY, nuclear Overhauser effect spectroscopy; TPPI, time-proportional phase incrementation; TSP, 3-(trimethylsilyl)[3,3,2,2-^{2}H]propionate-d_4.

S0006-2960(97)02288-5 CCC: $15.00
Published on Web 02/03/1998

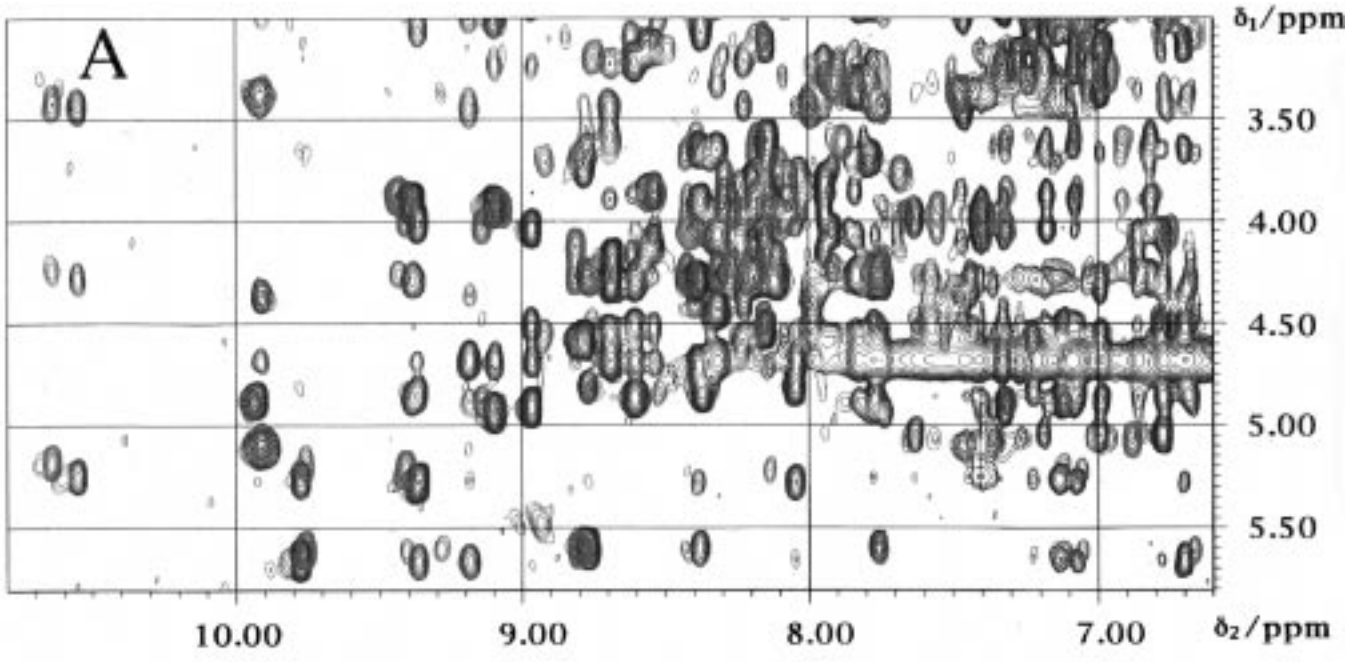
A
δ1/ppm
3.50
4.00
4.50
5.00
5.50
10.00
9.00
8.00
7.00
δ2/ppm

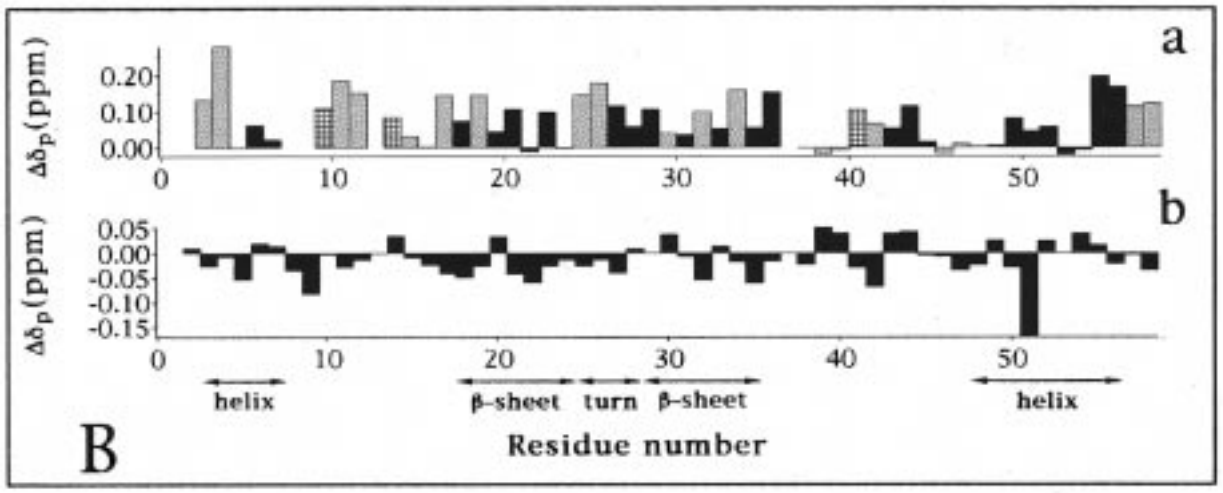
a
Δδp(ppm)
0.20
0.10
0.00
0
10
20
30
40
50
b
Δδp(ppm)
0.05
0.00
-0.05
-0.10
-0.15
helix
β-sheet
turn
β-sheet
helix
B
Residue number

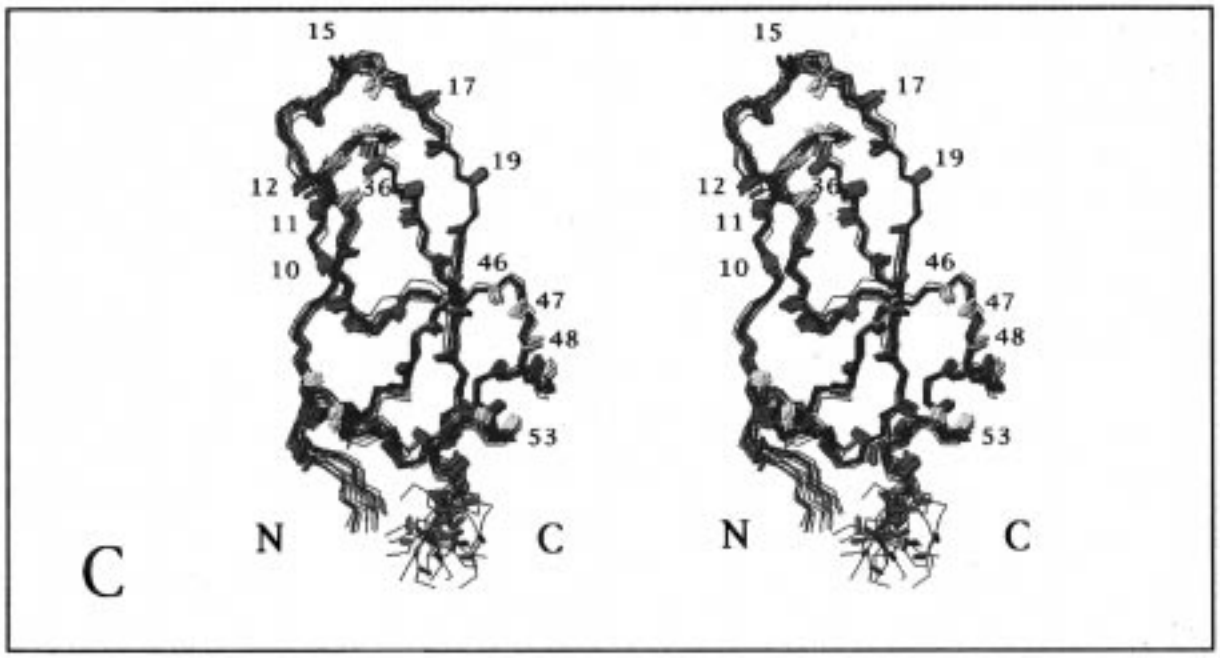
15
17
19
12
36
11
10
46
47
48
53
N
C
15
17
19
12
36
11
10
46
47
48
53
N
C
C

from cavities or voids produced by imperfect atomic packing within the tertiary structure (*5*, *6*, *17*, *18*).

In this report, we apply the same technique to an aqueous (90% ^1H_2O/10% ^2H_2O) solution of basic pancreatic trypsin inhibitor (BPTI) and focus our attention on the pressure effects on the labile hydrogens of the peptide NH groups. BPTI is a small globular protein consisting of 58 residues with three disulfide bridges (residues 5−55, 14−38, and 30−51) whose crystal and solution structures have been well-documented and known to be close to each other (*19*). This is also a protein for which high-pressure NMR was applied to find the pressure effect on rates of aromatic ring flips (*10*) and for which a molecular dynamic simulation was performed at high pressure (*20*).

MATERIALS AND METHODS

Sample Preparation. Crystals of BPTI (Sigma Chemical Co.) were dissolved into 90% ^1H_2O/10% ^2H_2O containing 200 mM buffer of acetate-d_3 (Isotec Inc.) to make a 10 mM solution of BPTI for NMR measurements. The pH of the solution was then adjusted to 4.6 by adding a small amount of NaOH or HCl.

High-Pressure NMR Apparatus. The high-resolution, high-pressure NMR technique employed here is a modification of the on-line high pressure glass tube method originally reported by Yamada (*21*). The protein solution is contained in a quartz tube (inner diameter of 1 mm, outer diameter of 3 mm, protected by a Teflon jacket), which is separated from the pressure mediator (kerosene) by a frictionless piston (Teflon) in a separator cylinder (BeCu). The pressure can be regulated at will between 1 and 2000 bar (measured with a Heise Bourdon gauge) with a hand pump remotely located from the 17.6 T magnet (Japan Magnet Technology), and is transmitted through a 6 m-long stainless steel tube containing kerosene to the sample solution in the NMR probe. A standard ^1H NMR probe for 5 mm sample tubes was used. The spectral resolution was excellent at any pressure, practically limited by intrinsic line widths.

NMR Measurements and Data Analysis. NMR spectra at various pressures were measured at 36 °C on a Bruker DMX-750 spectrometer operating at a proton frequency of 750.13 MHz. The NOESY spectra were obtained with spectral windows of 10 kHz with 256 complex points in the t_1 domain and 1024 complex points in the t_2 domain, using TPPI for phase-sensitive detection in the t_1 domain (*22*). Water suppression was accomplished by presaturation during the relaxation delay at high pressures or by using the pulsed field gradient WATERGATE technique (*23*) incorporating the 3−9−19 pulse sequence (*24*) at 1 bar. Chemical shifts were measured from the methyl signal of 3-(trimethylsilyl)[3,3,2,2-^2H]propionate-d_4 (TSP) at 0 ppm or from dioxane at 3.75 ppm, both added as internal references. The separation of the two signals was invariant with pressure within experimental error. A separate experiment showed that chemical shifts due to pH change of the solution [expected to be about −0.3 pH unit at 2000 bar for the acetate buffer (*25*)] were negligibly small.

Data were processed with the UXNMR package (Bruker) running on a Silicon Graphics Indigo2 workstation. The time domain data were zero-filled to 2048 and 1024 complex points in the t_1 and t_2 dimensions, respectively, and apodized using a quadratic sine-bell window function in both dimensions.

RESULTS

High-quality two-dimensional ^1H NMR NOESY (*26*, *27*) and TOCSY (*28*) spectra were obtained on BPTI in an aqueous environment (90% ^1H_2O/10% ^2H_2O and 200 mM acetate buffer at pH 4.6) at variable pressures between 1 and 2000 bar at 36 °C. ^1H NMR chemical shifts of practically all the protons were analyzed as functions of pressure. Most of the protons were found to undergo detectable shifts with pressure, and the shifts were linear and fully reversible with pressure; therefore, only data at 2000 bar will be analyzed below.

Figure 1A shows the fingerprint (NH−CαH) region of BPTI in which two NOESY spectra measured at 1 bar (green) and at 2000 bar (red) are superimposed. Each cross-peak represents the resonance position (chemical shift) of the Cα proton of the *i*th residue (ordinate) and that of the NH proton of the *i*th residue or the (*i*+1)th residue (abscissa), relative to the standard, the methyl proton resonance of (trimethylsilyl)propionate-d_4 (TSP). Clearly, we note that most cross-peaks undergo considerable shifts in both the NH and CαH axes at 2000 bar as compared to those at 1 bar. The spectral changes in Figure 1 are of an entirely different nature than those encountered in pressure-induced unfolding of proteins (*29*−*31*), and arise from changes in structure within the folded manifold. Since at 1 bar all the cross-peaks have been assigned to specific NH and Cα protons (except for the NH proton of Gly 37 and Arg 1) in the literature (*19*, *32*), these assignments could be easily extended to 2000 bar (red) by following spectra at intermediate pressures. We found that the cross-peaks shifted their positions nearly linearly with pressure up to 2000 bar, and these shifts were fully reversible.

The pressure-induced changes in chemical shifts [$\Delta\delta_P = \delta$(2000 bar) − δ(1 bar)] for the individual assigned amide and Cα protons are plotted as histograms in Figure 1B for

FIGURE 1: (A) Fingerprint (NH···CαH) regions of the NOESY spectra of BPTI, measured by using a Bruker DMX-750 spectrometer at 36 °C and at 1 bar (green) and 2000 bar (red). All the NH···CαH cross-peaks except for those of Arg 1 and Gly 37 out of 54 residues (58 residues minus 4 Pro residues) can be assigned to individual residues by referring to the literature (*32*). The sample of BPTI was dissolved to a concentration of 10 mM in 200 mM acetate-d_3 buffer in 90% ^1H_2O/10% ^2H_2O at pH 4.6. (B) Histograms of pressure-induced chemical shifts [$\Delta\delta_P = \delta$(2000 bar) − δ(1 bar)] for individual peptide NH and Cα protons of BPTI. (a) NH proton shifts at 36 °C [for 52 residues = 58 − 4 (Pro) − 1 (N-terminal amino of Arg 1) − 1 (unidentified NH of Gly 37)]. The filled columns are for the 28 NH protons hydrogen-bonded to carbonyls, the cross-hatched columns for the 4 NH protons hydrogen-bonded to internal water molecules which can be identified with X-ray diffraction, and the dotted columns for the 20 NH protons forming no hydrogen bonds to any of the above. (b) Cα proton shifts at 36 °C (for 57 residues except Arg 1). (C) Cross-eyed stereoview of the backbone atoms with positions and directions of the NH bonds, derived from 20 NMR structures (*19*) which were taken from the Brookhaven Protein Data Bank and drawn using the program MOLMOL. The NH bonds are colored into three groups with different ranges of the pressure-induced shifts ($\Delta\delta_P$) of the NH protons: $\Delta\delta_P > 0.09$ ppm (red), $0.03 < \Delta\delta_P < 0.09$ ppm (green), and $\Delta\delta_P < 0.03$ ppm (yellow).

(a) the amide protons and (b) the Cα protons. We notice clearly that, on average, shifts are much larger for the NH protons (an rms average of 0.101 ppm) than for the Cα protons (an rms average of 0.039 ppm). We also notice that the shifts of the NH protons occur preferentially to the lower field (positive $\Delta\delta_P$ values), while the Cα protons shift in both positive and negative directions. In all other proteins studied in our laboratory, including melittin (26 residues), gurmarin (*33*), hen egg white lysozyme, and cytochrome *c*, we found, without exception, a similar trend and magnitude of low-field shifts of the peptide NH protons with pressure (P. Dubovskii, K. Inoue, T. Tezuka, S. Ohji, Y. Kamatari, and K. Akasaka, unpublished experiments). These observations indicate that the tendency for low-field shifts with pressure is a general phenomenon for the peptide NH protons in proteins, irrespective of the type of amino acid, the primary sequence, the molecular weight, or the conformation of the protein.

DISCUSSION

The observation of the general tendency for the low-field shifts of NH protons in proteins with pressure indicates that the shift must be governed primarily by a mechanism common to all NH protons in various environments. To the authors' knowledge, pressure-induced low-field shifts of hydrogen-bonded protons have been shown only in simple protic liquids such as water and alcohol (*34*, *35*). There, the low-field shifts are attributed to the compression of the liquids and therefore to the shortening of the hydrogen bonds. The low-field shifts of the peptide NH protons should share essentially the same mechanism as those (*36*). Namely, the chemical shift of the NH proton must be due to compression of the hydrogen bond, and is determined primarily by the local electronic structure of the hydrogen bond; i.e., a shorter H···O distance corresponds to a stronger polarization of the hydrogen bond, and hence less shielding of the magnetic field, leading to a lower field shift for the proton.

We further recognize in Figure 1B (part a), however, that the magnitude of the shift varies considerably from residue to residue, some shifts being close to null or even going to high field. BPTI contains two small helixes (residues 3−7 and 47−56), a β-sheet (residues 18−24 and 29−35), a turn (residues 25−28), and loops for the rest of the structure as shown in Figure 1 (*19*), but there appears no simple correlation between the shifts and the secondary structures as a group. We then look into shifts of individual NH protons and classify them according to their hydrogen bonding partners: those hydrogen-bonded to carbonyl oxygens (forming secondary structures; 28 filled columns), those hydrogen-bonded to the internal waters [4 cross-hatched columns (10, 14, 38, and 41)], and those that form no detectable hydrogen bonding by X-ray diffraction at room temperature (the "free" NH groups; 20 dotted columns). Here, we find an interesting tendency that the shifts of the free NH protons (dotted columns) are more sensitive to pressure (an average shift of 0.098 ± 0.079 ppm/2 kbar) than those hydrogen-bonded to carbonyls (filled columns; an average shift of 0.059 ±0.056 ppm/2 kbar). The high sensitivity of the free NH groups to pressure suggests that they are not actually free but are hydrogen-bonded to solvent water and that these hydrogen bonds are shortened by pressure. This interpretation apparently contradicts the conclusion from the molecular dynamics simulation that no pressure-induced shortening of the NH···water hydrogen bonds takes place (*20*), but if we consider the resolution of the molecular dynamic simulation (ca. ±0.1 Å) and in our high-pressure NMR (ca. ±0.001 Å, as we see later), the two results are not contradictory.

We further recognize in Figure 1B (part a) that among the same classes of hydrogen bonding, e.g., among the free NH group itself, there is a sizable variation in magnitude of shifts. To find origins for individual variations of the shifts, we need to look more closely into individual hydrogen bonding states of NH groups. We divided the NH groups into three grades (1−3) according to the magnitude of pressure-induced shifts ($\Delta\delta_P$), and located them by marking them with colors on the tertiary structure of BPTI determined by NMR in solution (*19*) (Figure 1C): (1) $\Delta\delta_P > 0.09$ ppm (red), (2) $0.03 < \Delta\delta_P < 0.09$ ppm (green), and (3) $\Delta\delta_P < 0.03$ ppm (yellow). Here, we notice an interesting correlation between the magnitudes of the shifts and the locations of the NH groups. First, the NH protons giving the largest shifts (red) are found in the apparently fraying N-terminal (residues 3 and 4) and C-terminal segments (residues 55−58) and in the loop region (residues 10−12) where the NH groups are pointing outward to the solvent. We also find in the β−sheet region (residues 18−35) the red NH groups in alternating order (residues 17, 19, 21, 23, 32, 34, and 36), all directed outward. In the same β−sheet region, those in green also alternate in number (18, 20, 22, 24, 31, 33, and 35), but all are directed inward (to form interstrand hydrogen bonds as required by a β-sheet topology). These observations clearly show the tendency that those NH groups directed outward are the ones experiencing the largest shifts (the average shift for these is 0.129 ppm/2 kbar). They are exposed to the solvent and probably form most favorable hydrogen bonds with the surrounding water molecules.

Evidence supporting this view is obtained from the cryogenic crystallography performed on BPTI (*37*). We find that many NH groups colored in red in Figure 1C (residues 3, 10−12, 19, 25, 32, 34, 41, and 57) have in the crystal favorable hydrogen bonds with water (N···O distance of <3.1 Å), although such water molecules were not detected for other red-colored groups (residues 17, 21, 23, and 36). In contrast, the shifts of most of the inwardly directed NH protons in the turn regions (38−40, 45, and 46) showed very small shifts (yellow), presumably due to unfavorable hydrogen bonding with the solvent. More supporting evidence comes from measurement of pressure-induced shifts of a typical unfolded polypeptide chain of 26 residues, melittin in water at low pH, whose peptide NH protons are likely to form favorable hydrogen bonds with water. The result indicates that in this case the pressure-induced shifts occur much more uniformly over the entire polypeptide chain, as expected, and that the average shift is 0.108 ppm/2 kbar (P. Dubovskii and K. Akasaka, unpublished experiments). All the above observations support the notion that a favorable hydrogen bonding with water is a major condition leading to the high sensitivity of an NH proton chemical shift to pressure, going approximately to the level of 0.10 ppm/2 kbar. From these results, it is suggested that the pressure-induced shifts of the water-hydrogen-bonded NH protons

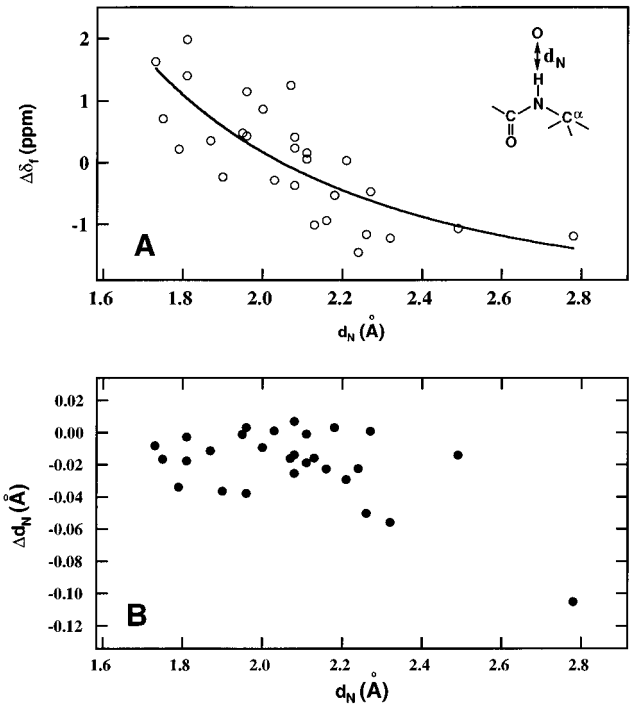

FIGURE 2: (A) Plot of the formation shift against the H···O distance (d_N) of the NH···O═C hydrogen bond in BPTI. (B) Plot of the estimated pressure-induced shortening of the H···O distance (Δd_N) against the H···O distance (d_N) of the NH···O═C hydrogen bond in BPTI.

may be used for probing microscopic interaction of the hydrophilic NH groups of a protein with solvent water.

We may further ask how much the actual shortening of individual hydrogen bonds of BPTI can be. Using the geometries of the NH···O═C hydrogen bonds of BPTI at 1 bar known in the crystal structure, Wagner et al. (*38*) found that, for these NH protons, the hydrogen bond "formation shift" ($\Delta\delta_f$), defined here as the observed shift in the folded state (δ_{obs}) minus the ring current shift and minus the random coil shift (δ_{rc}), correlated well with the H···O distance (d_N) of the NH···O═C hydrogen bond. In Figure 2A, we plot the formation shifts determined at 750 MHz and 1 bar against the H···O distances (d_N) of 28 NH···O═C hydrogen bonds in the crystal (*19*). We observe in Figure 2A that, as the H···O distance varies in the crystal considerably, so does the folding shift, with a clear trend where the shorter the d_N, the more low-field the formation shift. The least-squares fit to this plot (represented by the thick line in Figure 2A) essentially confirmed the relationship obtained earlier by Wagner et al. (*38*, *39*), with a slight modification of the parameters, i.e.,

$$\Delta\delta_f = 19.9 d_N^{-3} - 2.3 \quad (1)$$

The relatively strong correlation (correlation coefficient of 0.77) appears to indicate that other factors such as the contribution from the hydrogen bonding state of the carbonyl group directly bonded to the amide group (*40*) do not play crucial roles in determining the amide proton shift. Similar shift−distance correlations have been found more recently in many other proteins (*41*).

Equation 1 depicts an approximate dependence of the H···O hydrogen bond distance d_N on the chemical shift $\Delta\delta_f$ for any of the NH···O═C groups in BPTI. If the formation chemical shift $\Delta\delta_f$ of an NH proton with a distance d_N is changed further by $\Delta\delta_P$ by pressure within the folded manifold of BPTI, we expect that its d_N has changed to a new value approximately according to eq 1. Magnitudes of shortening of d_N at 2000 bar were estimated in this way for the 28 individual NH protons of BPTI from the observed pressure-induced shifts ($\Delta\delta_P$), and are plotted against original distances at 1 bar in Figure 2B. The magnitudes of shortening range from +0.01 Å (slight elongation) to −0.11 Å (a considerable shortening), the average being −0.020 Å which corresponds to a shortening of d_N of about 1%. The plot also depicts some tendency where the larger the H···O distance d_N, the larger its shortening; i.e., the longer the hydrogen bond, the greater the compression, which appears to be reasonable.

Estimated shortenings for individual H···O bonds of 28 NH···O═C hydrogen bonds are plotted against the amino acid sequence in Figure 3. The result predicts the largest

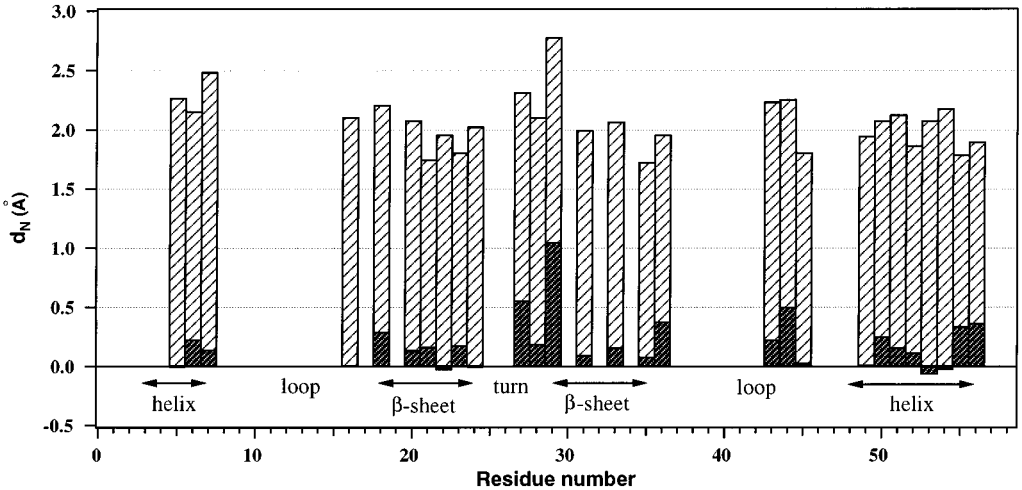

FIGURE 3: Estimated shortenings of the individual H···O hydrogen bond distances at 2000 bar (the darkly cross-hatched columns, values were magnified by 10 times). The plots were made for those NH groups forming hydrogen bonds with carbonyl groups, i.e., NH···O═C, in the crystal structure of BPTI (*19*) and were estimated from the experimental pressure-induced shifts and eq 1 (see the text for more details). The lightly cross-hatched columns represent H···O hydrogen bond distances at 1 bar.

compression in the turn region (residues 27−29) and in the peripheral parts (residues 18 and 36) of the β-sheet and of the helix (residues 50, 55, and 56). Less compression is predicted for the interior regions of the β-sheet (residues 20−24) and the helix (residues 51−54). To the authors' knowledge, the result demonstrates, experimentally for the first time, that compression occurs in hydrogen bonds in a protein. It also adds new insight into the origin of macroscopic compressibility of a globular protein, for which the hitherto accepted notion has been that the compression occurs only in cavities primarily due to imperfect side chain packing (*5*, *6*). The result also demonstrates that the compression is not uniform within the hydrogen-bonded network of a protein.

Since all the observed pressure-induced shifts were linear with pressure up to 2000 bar, the compression at 2000 bar can be linearly extrapolated to 1 bar. Hence, from the general relation between the compressibility and the volume fluctuation (*42*), the nonuniform compressibility of the hydrogen bonds shown in Figure 3 may be considered part of the microscopic volume fluctuation of BPTI. Namely, it predicts that the fluctuation is higher in the turn region and in the peripheral regions of the β-sheet and the helix than in the interior parts of the β-sheet and the helix. This example illustrates a novel way to study microscopic structural fluctuation of a protein molecule experimentally. It should be recognized that this method is sensitive to such structural fluctuation as to contribute to volume fluctuation and therefore is differently biased from those fluctuations obtainable from X-ray *B*-factors and NMR relaxation. It appears to be particularly sensitive to subtle fluctuation in hydrogen bonds as well as fluctuation in side chain packing in the interior part of the protein (*16*). In fact, the NH proton shift by a few hertz corresponds to a shortening of the hydrogen bond by only 0.001 Å.

The Cα protons [Figure 1B (part b)] as well as most side chain protons (data not shown) also showed considerable shifts with pressure. These shifts should be intimately related to the secondary and tertiary structural changes, which is another interesting aspect of the pressure effect on proteins (*16*). This subject will be treated in more detail elsewhere.

CONCLUDING REMARKS

We found that the H···O distances of the individual hydrogen bonds of BPTI are shortened by different degrees at high pressure. For the NH groups internally hydrogen-bonded to carbonyls, the degree of shortening varies from site to site, with a slight tendency being that the longer the hydrogen bond, the greater the shortening. For the NH groups externally hydrogen-bonded with solvent water, their chemical shifts are particularly sensitive to pressure, the magnitudes of which apparently reflect the microscopic hydrogen bonding states of water with individual NH groups. Since all the observed shifts are linear and reversible with pressure in the pressure range investigated (1−2000 bar), the high-resolution, high-pressure NMR technique employed here will provide a novel experimental approach for detecting microscopic volume fluctuation, or structural fluctuation at atomic resolution, of a protein at ordinary pressure.

REFERENCES

1. Weber, G. (1975) *Adv. Protein Chem. 29*, 1−85.
2. Taniguchi, Y., and Suzuki, K. (1983) *J. Phys. Chem. 87*, 5185−5193.
3. Markley, J. L., Northrop, D. B., and Royer, C. A., Eds. (1996) *High-Pressure Effects in Molecular Biophysics and Enzymology*, Oxford University Press, Oxford, England.
4. Hayashi, R., and Balny, C., Eds. (1996) *High-Pressure Bioscience and Biotechnology*, Elsevier, Amsterdam.
5. Gekko, K., and Hasegawa, Y. (1979) *J. Phys. Chem. 83*, 2706−2714.
6. Gekko, K., and Hasegawa, Y. (1986) *Biochemistry 25*, 6563−6571.
7. Hawley, S. A. (1971) *Biochemistry 10* (13), 2436−2442.
8. Zipp, A., and Kauzmann, W. (1973) *Biochemistry 12* (21), 4217−4228.
9. Takeda, N., Kato, M., and Taniguchi, Y. (1995) *Biochemistry 34*, 5980−5987.
10. Wagner, G. (1980) *FEBS Lett. 112*, 280−284.
11. Morishima, I. (1987) in *Current Perspectives of High-Pressure Biology*, pp 315−333, Academic Press.
12. Peng, X., Jonas, J., and Silvia, L. (1993) *Proc. Natl. Acad. Sci. U.S.A. 90*, 1776−1780.
13. Urbauer, J. L., Ehrhardt, M. R., Bieber, R. J., Flynn, P. F., and Wand, A. J. (1996) *J. Am. Chem. Soc. 118*, 11329−11330.
14. Kundrot, C. E., and Richards, F. M. (1987) *J. Mol. Biol. 193*, 157−170.
15. Yamada, H., Nishikawa, K., Sugiura, M., and Akasaka, K. (1997) *International Conference on High-Pressure Science and Technology*, Abstracts, p 413, The Japan Society of High Pressure Science and Technology, Kyoto.
16. Akasaka, K., Tezuka, T., and Yamada, H. (1997) *J. Mol. Biol. 271*, 671−678.
17. Lee, B., and Richards, F. M. (1971) *J. Mol. Biol. 55*, 379−400.
18. Frauenfelder, H., Hartmann, H., Karplus, M., Kuntz, I. D., Jr., Kuriyan, J., Parak, F., Petsko, G. A., Ringe, D., Tilton, R. F., Jr., Connolly, M. L., and Max, N. (1987) *Biochemistry 26*, 254−261.
19. Berndt, K. D., Guntert, P., Orbons, L. P. M., and Wuthrich, K. (1992) *J. Mol. Biol. 227*, 757−775.
20. Kitchen, D. B., Reed, L. H., and Levy, R. M. (1992) *Biochemistry 31*, 10083−10093.
21. Yamada, H. (1974) *Rev. Sci. Instrum. 45*, 640−642.
22. Marion, D., and Wuthrich, K. (1983) *Biochem. Biophys. Res. Commun. 113*, 967−974.
23. Piotto, M., Saudek, V., and Sklenar, V. (1992) *J. Biomol. NMR 2*, 661−665.
24. Sklenar, V., Piotto, M., Leppik, R., and Saudek, V. (1993) *J. Magn. Reson., Ser. A 102*, 241−245.
25. Isaacs, N. S. (1981) *Liquid-Phase High-Pressure Chemistry*, Chapter 3, John Wiley & Sons, New York.
26. Jeener, T., Meier, B. H., Bachmann, P., and Ernst, R. R. (1979) *J. Chem. Phys. 71*, 4546−4553.
27. Macura, C., Huang, Y., Suter, D., and Ernst, R. R. (1981) *J. Magn. Reson. 43*, 259−281.
28. Braunschweiler, L., and Ernst, R. R. (1983) *J. Magn. Reson. 53*, 521−528.
29. Royer, C. A., Hinck, A. P., Loh, S. N., Prehoda, K. E., Peng, X., Jonas, J., and Markley, J. L. (1993) *Biochemistry 32*, 5222−5232.
30. Jonas, J., and Jonas, A. (1994) *Annu. Rev. Biophys. Biomol. Struct. 23*, 287−318.
31. Yamaguchi, T., Yamada, H., and Akasaka, K. (1995) *J. Mol. Biol. 250*, 689−694.
32. Wagner, G., Braun, W., Havel, T. F., Schaumann, T., Go, N., and Wuthrich, K. (1987) *J. Mol. Biol. 196*, 611−639.
33. Arai, K., Ishima, R., Morikawa, S., Miyasaka, A., Imoto, T., Yoshimura, S., Aimoto, S., and Akasaka, K. (1995) *J. Biomol. NMR 5*, 297−305.
34. Linowski, J. W., and Jonas, J. (1976) *J. Magn. Reson. 23*, 455−460.
35. Linowski, J. W., and Jonas, J. (1976) *J. Chem. Phys. 65*, 3383−3384.

36. Buckingham, A. D. (1960) *Can. J. Chem. 38*, 300−307.
37. Parkin, S., Rupp, B., and Hope, H. (1995) Protein Data Bank (1BPI), Brookhaven National Laboratory, Upton, NY.
38. Wagner, G., Pardi, A., and Wuthrich, K. (1983) *J. Am. Chem. Soc. 105*, 5948−5949.
39. Pardi, A., Wagner, G., and Wuthrich, K. (1983) *Eur. J. Biochem. 137*, 445−454.
40. Llinas, M., and Klein, M. P. (1975) *J. Am. Chem. Soc. 97*, 4731−4737.
41. Asakura, T., Taoka, K., Demura, M., and Williamson, M. P. (1995) *J. Biomol. NMR 6*, 227−236.
42. Cooper, A. (1976) *Proc. Natl. Acad. Sci. U.S.A. 73*, 2740−2741.

BI972288J